COMMISSIONING OF A CENTRALIZED COOLING PLANT

by F. BILAS, J-P. BOURDOUXHE, B. GEORGES, H. HU,
V. JENNES, J. LEBRUN, J.M. PIMENTA

University of Liège, Laboratory of Thermodynamics

1 . ABSTRACT

The centralized cooling plant considered equips an important office building in Brussels. This 54 000 m^2 building has a design cooling demand of about 5.7 MW. To meet the cooling loads, the chilling plant can use five counterflow cooling towers, four twin-screw chillers and four tanks with encapsulated ice.

The purpose of the commissioning is to check the thermal performance of the primary equipment and to use the simulation tools to give a correct forecast of the cooling capacity available as well as the cooling energy stored in the ice storage tanks.

The cooling plant has been operating for three years. Therefore, this commissioning has been submitted to two important constraints : the freedom to test the chilling plant in various configurations is very limited and one can only deal with the information provided by the BEMS (Building & Energy Management System) and the control display of the chillers.

Since no flow meter equips the cooling plant, a series of energy and mass balances based on the data provided by the acquisition system are done. The analysis of these data points out the inaccuracy of several temperature sensors. As a result, this inaccuracy is transferred to the flow rates given by the energy balances (especially at low cooling loads).

To overcome partially this problem, a hydraulic analysis of the cooling plant is done thanks to the data provided by the installers.
The flow rates given by the hydraulic simulation and the data provided by the control panels of the chillers are then used to evaluate the thermal performance of the chillers.

These results are confronted with the results of the simulation of the chillers. Such as for the other components of the cooling plant, the model of chiller is identified on the basis of the information given by the manufacturer.

The whole centralized cooling plant can also be simulated in all its operating modes. The paper shows how the simulation of one of these modes, the discharging, is validated.

2. BUILDING AND COOLING PLANT DESCRIPTION

The cooling plant analyzed in this paper is equipping the building of the Ministry Council of the European Union in Brussels. This building is built on a 40 000 m^2 ground area, with about 54 000 m^2 of useful area, distributed on 10 floors. The whole building is composed of two main parts : the Conference building (25 000 m^2) and the General Secretariat (29 000 m^2) (see Figure 1).

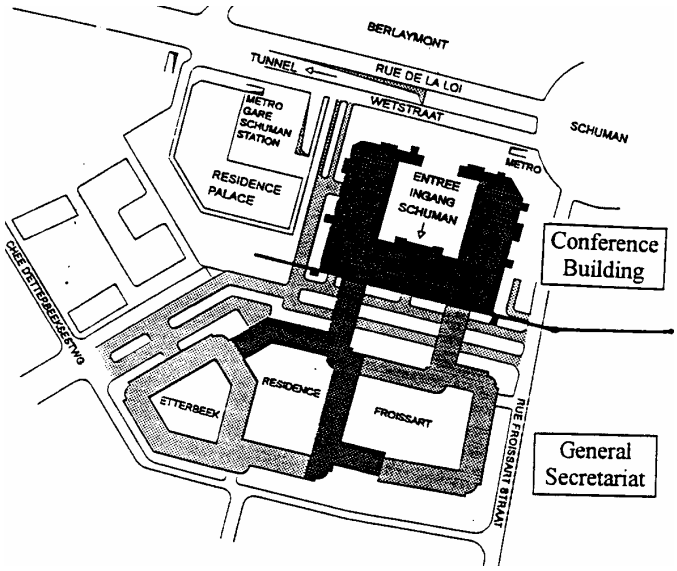

Figure 1 - Horizontal View of the Whole Building Situation.

The Conference building, shown in Figure 2, is the higher part of the site, being distributed on 7 floors and 3 mezzanines. It mainly includes meeting rooms with interpreter cabins, conference and ceremonial rooms and delegation offices, but also three restaurants and one cafeteria. The maximal occupancy is about 3 500 persons, and the nominal cooling loads are about 4 MW (outside temperature = 30 °C; outside relative humidity = 50%).

Figure 2 - The Conference Building.

The General Secretariat building is organized all around four large patios, allowing a natural lighting of all the rooms. It is connected to the Conference building by two "wings". Its height goes down in terraces from 9 to 7 floors. This building includes mainly offices, printing rooms and computer room. There are also a sport area and a cafeteria. The maximal occupancy is about 2 500 persons and the nominal loads are about 1.7 MW.

The whole plant is designed to be able to meet a building cooling loads of 5.7 MW (outside air wet-bulb temperature : 22 °C).
The technical solution adopted in order to meet the building cooling loads is to use an ice storage system operating in parallel with the chillers. This allows one to reduce the number and the size of chillers, as well as to take advantage of the reduced cost of electricity during the night when the storage tanks are charged (ASHRAE, 1995). A simplified view of the centralized cooling plant is shown in Figure 3.

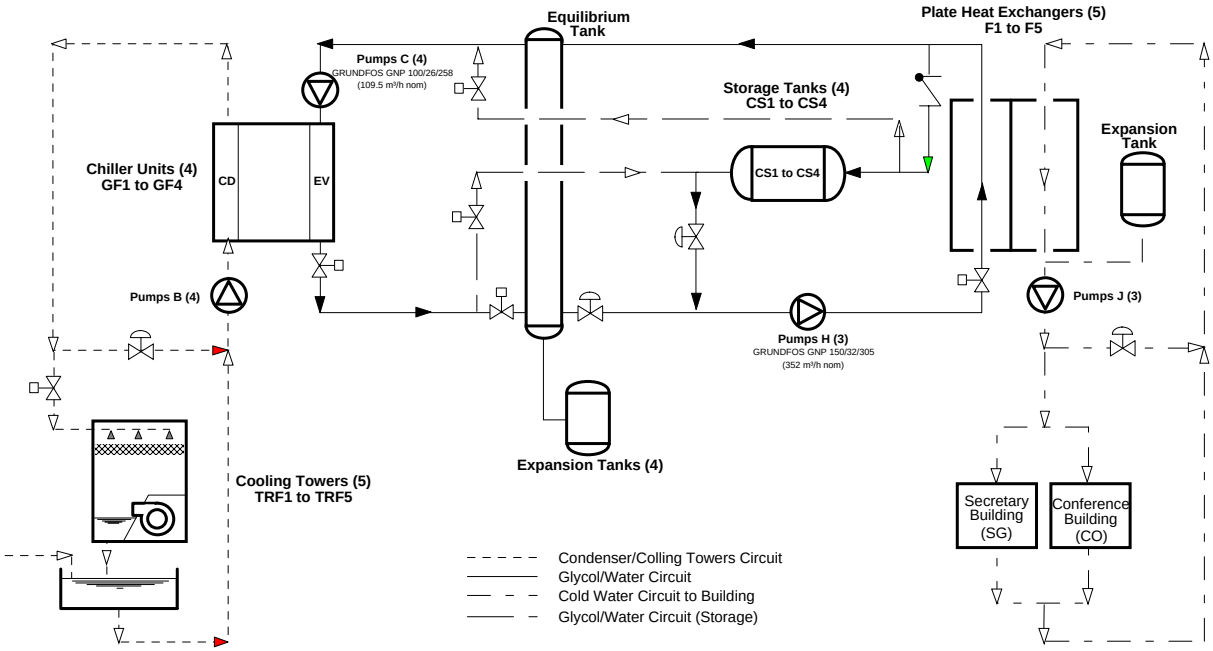

Figure 3 - Simplified schematic view of the cooling plant.

The plant operates thanks to the adequate set-up of the following main components :

- Five counterflow plate heat exchangers in parallel arrangement;
- Four horizontal encapsulated ice storage tanks in parallel-series arrangement;
- An equilibrium tank that equilibrates the pressures between the chillers evaporators, the ice storage tanks and the heat exchangers. Due to the different flow rates in the evaporators and in the heat exchangers, a bypass of a fraction of the plate heat exchanger flow rate will occur inside the equilibrium tank, resulting in a temperature increase at the equilibrium tank exhaust (plate heat exchanger side);
- Four R22 twin-screw chillers in parallel arrangement. Capacity control is achieved thanks to a slide valve which can modulate the chiller capacity from 100 % down to about 10 % of full-load. Each chiller has a fixed-speed pump on the evaporator and condenser sides.
- Five counterflow cooling towers in a parallel arrangement. Each tower is equipped with a two-speed centrifugal fan.

All these components are inter-connected by three networks :

- The chilled water distribution network to buildings. It is characterized by three fixed-speed pumps (called hereafter “secondary” pumps) and a bypass which controls, thanks to modulating valves, the water flow supplied to the building;
- The glycol water circuit on evaporator and ice storage tank side. It is characterized by three fixed-speed pumps (called hereafter “primary” pumps) and two modulating valves which control the flow in the ice storage tanks and in the equilibrium tank;
- The warm water circuit on condenser side. It includes a reservoir where the make-up water is added, and a bypass which avoids, thanks to a modulating valve, a too low temperature at the condenser supply.

Depending on the overall building demand, the plant can be configured to operate in *priority* according one of the following three modes :

1. Direct Production mode : The expected total building demand is quite high (above the maximum storable energy in the storage tanks). In this case, the four chillers will be operating in priority, with an eventual discharge from the storage tanks, if the four chiller refrigerating capacity is not sufficient.
2. Storage Tank Discharging mode : The expected total building demand is moderate (below the maximum storable energy in the storage tanks), allowing to carry out a discharge of the storage tanks in priority, with an eventual direct production by one or more chillers.
3. Storage Tank Charging mode (called hereafter storage mode) : The energy currently stored in the tanks is not sufficient for the operation on one of the two modes above, so that, it is necessary to run the plant in order to charge the tanks in priority. A particularity of this building is that, even in charging mode, the cooling plant has always to meet a non-negligible cooling demand.

The whole HVAC system is permanently monitored by a BEMS (Building and Energy Management System) which receives indication from sensors placed at the main system points, and actuates on the different control devices and whose purpose is to maintain the chilled water temperature at 7 °C with a pressure drop of 180 000 Pa through the building. The information about the cooling plant provided by the BEMS can be classified into three categories (see Figure 4) :

- Physical measurements : they are temperatures, differential pressure and building energy demand. Temperatures and differential pressure are identified by codes like ENF004_ _ _M_ _ (see Figure 4), while the energy demand is represented by codes like ENF004_ _ _Z_ _. All the temperature sensors are installed in "glove-finger" arrangements;
- Control commands : they are signals sent by the BEMS to the plant in order to change the state of a specific device. The changes can be discontinuous (open/close, on/off, high/low, etc. ; identified by codes like ENF004_ _ _C_ _.) or continuous (for the modulating control valves ; identified by codes like ENF004_ _ _R_ _) ;
- Regulation variables : they are the set point on temperatures (e.g. at the evaporator exhaust and at the building supply) and on pressure as well as upper and lower temperature limits (e.g. lower water temperature limit at the condenser supply).

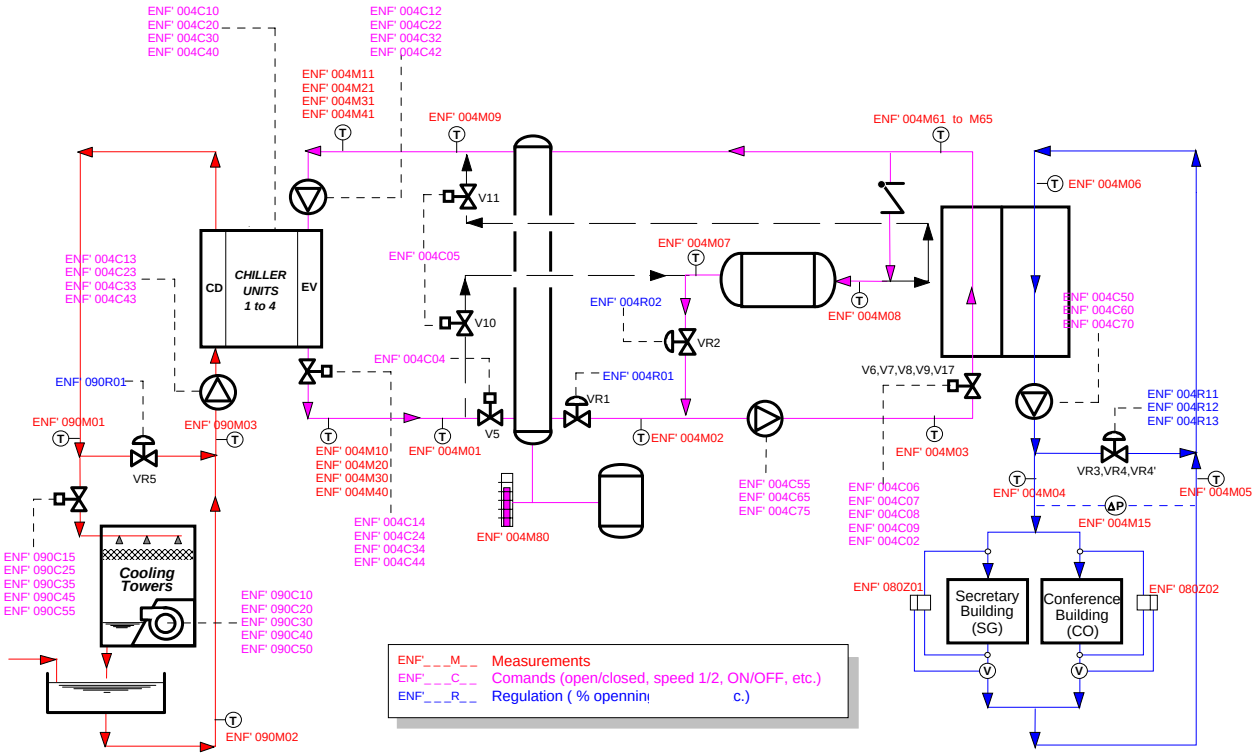

Figure 4 : Data provided by the BEMS

Some local instrumentation (not connected to the BEMS) is also available : each chiller is furnished with a factory-mounted micro-computer control center including an alphanumeric display showing the following operating information :

- current date and time;
- Set-point at the evaporator exhaust;
- condensing pressure;
- condenser water supply temperature;
- condenser water exhaust temperature;
- evaporating pressure;
- evaporator water-glycol supply temperature;
- evaporator water-glycol exhaust temperature;
- compressor refrigerant exhaust temperature;
- compressor lubricant temperature;
- a variable function of the compressor slide valve opening;
- motor full load current ratio.

In order to take advantage of this information, a PC data acquisition facility is connected to the existing chiller communication interface. It allows one to store all the available operating data from the chillers sensors, for off-line analysis.

All this information represents an impressive amount of data.. However, a very important data is missing : the flow rates. Indeed, no flow meter is installed in the chilling plant. The only information about flow rate are the chilled water flow rates given by two enthalpy flow meters installed on the chilled water distribution of the buildings. But this information is not handled by the BEMS.

Due to the fact that the cooling plant has been operating for three years, the interventions on the

equipment (installation of measurement devices or testing of the chilling plant in various configurations) are very limited. As a result, the information provided by the BEMS and the control display of the chillers is the only information one can deal with.

3. MEASUREMENT ANALYSIS AND THERMAL AND MASS BALANCES

Since no flow meter equips the cooling plant, a series of energy and mass balances based on the temperatures provided by the acquisition system and the cooling loads "measured" by the enthalpy flow meters is done.
In theory, these thermal and mass balances should allow the determination of the water and glycol water flow rates and the evaluation of the thermal performances of the plant components.
But they also point out the inaccuracy of some sensors. Moreover, at low building cooling loads, even a normal inaccuracy of the sensors leads to a very inaccurate determination of the flow rates.
As a result, the thermal and mass balances are of limited use and must be completed by a hydraulic analysis of the water and glycol water circuits.

The data acquisition system provides the fluid temperature at the supply and exhaust of most components of the chilling plant. Comparing the temperature at the exhaust of one component with the temperature at the supply of the following one allows one to check whether both temperature sensors are in good agreement.
This method gives a second way to check the accuracy of the sensors. It also points out the inaccuracy of a few sensors.

4. HYDRAULIC ANALYSIS OF THE CENTRAL PLANT

To evaluate more precisely the flow rates, the warm water and the glycol water circuits are simulated.
To model these circuits, the pressure drop through a component crossed by the mass flow rate $\dot{M}$ is given by :

$$\Delta p = K \dot{M}^2 \qquad (1)$$

where K is the pressure drop coefficient ($kg^{-1}\ m^{-1}$), assumed to be constant (except for the modulating valves)

The results of the hydraulic simulation is used in the simulation of the thermal performance of the cooling plant and its components.

4.1. The warm water circuit

The determination of the pressure drop coefficients associated with the components of this circuit (cooling towers, condensers, pipes, etc.) is based on geometric description of the plant, performance curves of the condenser pumps, on-site measurements and data provided by the installators and equipment manufacturers (Jennes, 1996).
Once the pressure drop coefficients are known, the water mass flow rates can be calculated. The water flow rate distribution among the chillers and among the cooling towers is assumed to be uniform.

Table 1 gives the simulated total water mass flow rate in the condensers as a function of the number of operating chillers and the opening ratio of the tower bypass valve.

Table 1 : simulated total water mass flow rate in the condensers (number of towers = number of chillers + 1)

By-pass valve (%)	total water mass flow rate in the condensers (kg/s)			
	1 chiller	2 chillers	3 chillers	4 chillers
0	70	127	170	198
50	74	139	186	213
100	77	145	197	223

The nominal condenser pump flow rate is equal to 54 kg s^{-1}. The hydraulic simulation gives therefore a water flow rate per condenser higher than the nominal value, except when fours chillers are used with a bypass valve opening ratio lower than 50 %.

4.2. The glycol water circuit

The determination of the pressure drop coefficients through the different components (evaporators, plate heat exchangers, etc.) is based on the information provided by the installators (CEE-CLIM, 1995a and 1995b).
However, two important data are not supplied : the characteristics of the modulating valves at the storage tank exhaust and at the equilibrium tank exhaust, and the pressure drops in the storage tanks for any configuration.
Therefore, the characteristics of the valves are defined by analogy with the characteristics of the cooling tower bypass valve, and the pressure drop through the storage tanks is assumed to be defined only on the basis of the few data available.

The uncertainty on the valve characteristics leads to a important uncertainty on the flow rates when the valve opening ratios are low, i.e. when the valve authority is great.

Two plant operating modes must be considered when simulating the flow rates : the direct production mode with/without discharge, and the storage mode.

In the direct production mode, the evaporator circuit is assumed to be isolated from the storage tank and plate heat exchanger circuit by the equilibrium tank (see Figure 5-a). In this case, the flow rate per evaporator only depends on the number of operating chillers. It is also assumed that the glycol water flow rate is uniformly distributed among the operating chillers.

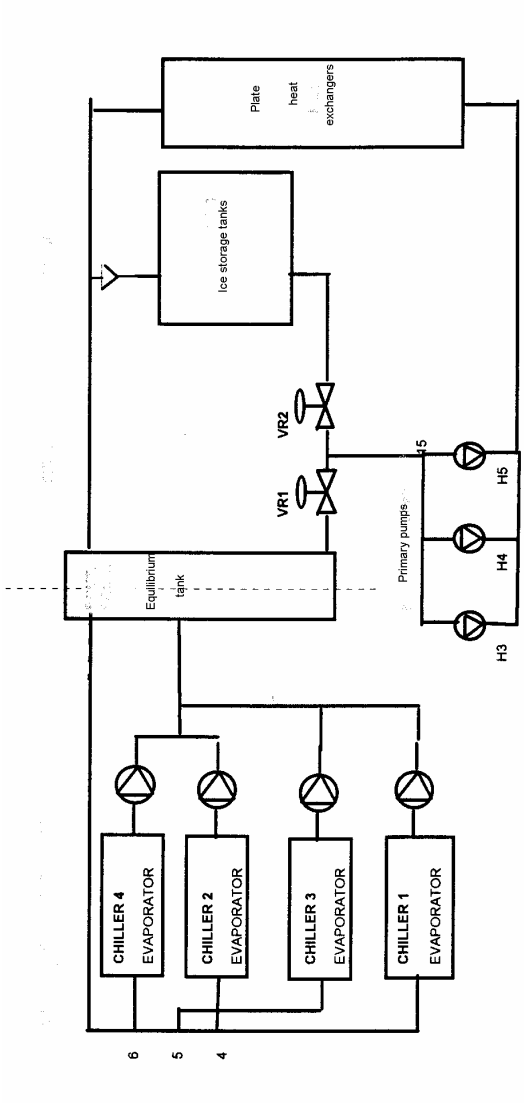

Figure 5-a : direct production mode with/without discharge

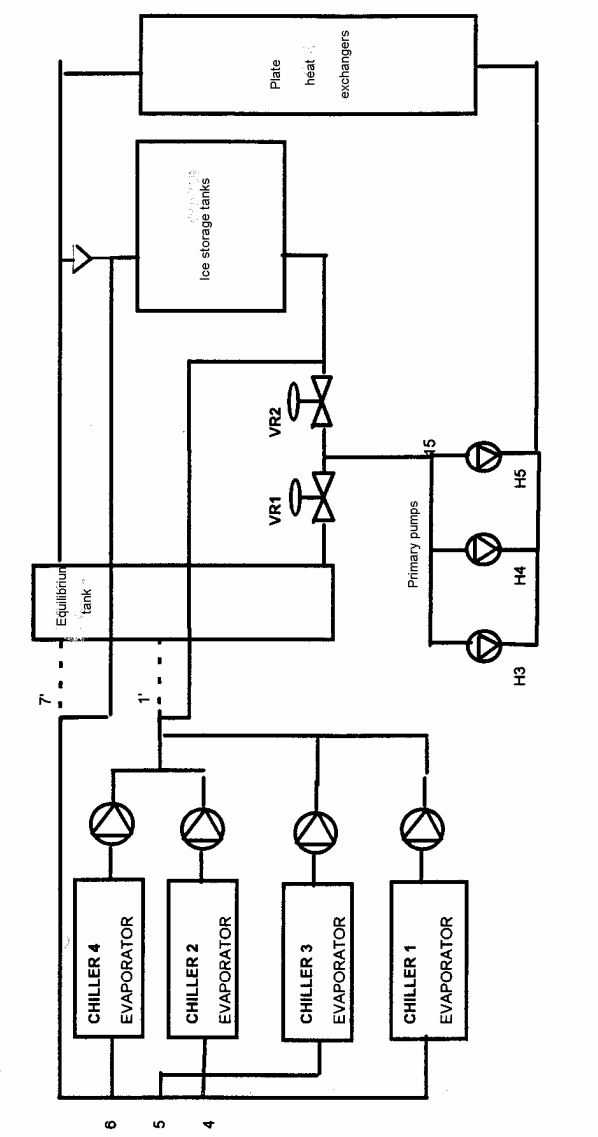

Figure 5-b : storage mode with direct production

Table 2 gives the simulated glycol water mass flow rate per evaporator as a function of the number of operating chillers.

Table 2 : simulated glycol water mass flow rate per evaporator in direct production mode

Nr. chillers	flow rate (kg/s)
1	40.5
2	39
3	36.9
4	34.5

The evaporator glycol water mass flow rate is also calculated, for one and two operating chillers, on the basis of the thermal balances. These flow rates are equal to 42.3 kg s^{-1} and 36.3 kg s^{-1} respectively for one and two operating chillers. As can be seen, they are in satisfactory

agreement with the results of the hydraulic simulation.
During a discharging test at high cooling loads, a few reliable thermal balances have been done. Table 3 compares the total glycol water flow rate in the plate heat exchangers given by the thermal balances and by the hydraulic simulation.

Tableau 3 : Comparison between the total glycol water flow rate in the plate heat exchangers given by thermal balances and by hydraulic simulation (valve VR1 at 80 %)

	Thermal balances			Hydraulic simulation		
	1st data	2nd data	3rd data	1st data	2nd data	3rd data
Opening ratio VR2 (%)	50	80	100	50	80	100
Total glycol water flow rate in plate heat exchangers (kg/s)	207.5	189.5	**194.9**	251.8	254.4	**255**

On the basis of the results of these thermal balances, the simulation of the flow rates in the storage tanks and the plate heat exchanger is then roughly adjusted
The third data is used as reference to adjust the results given by the hydraulic simulation. This means that the simulated glycol water flow rates in the ice storage tanks and in the plate heat exchangers are multiplied by the following coefficient k_m :

$$k_m = \frac{flow\,rate\ from\,thermal\,balance\,(3rd\,data)}{flow\,rate\ from\,hydraulic\,simulation\,(3rd\,data)} = \frac{194.9}{255} = 0.7643$$

This adjustment is also roughly assumed to be valid in storage mode. In this mode, the evaporator circuit is no more independent from the storage tank and plate heat exchanger circuit (see Figure 5-b). The glycol water mass flow rate per evaporator is thus also function of the modulating valve opening ratios (see Figure 6).

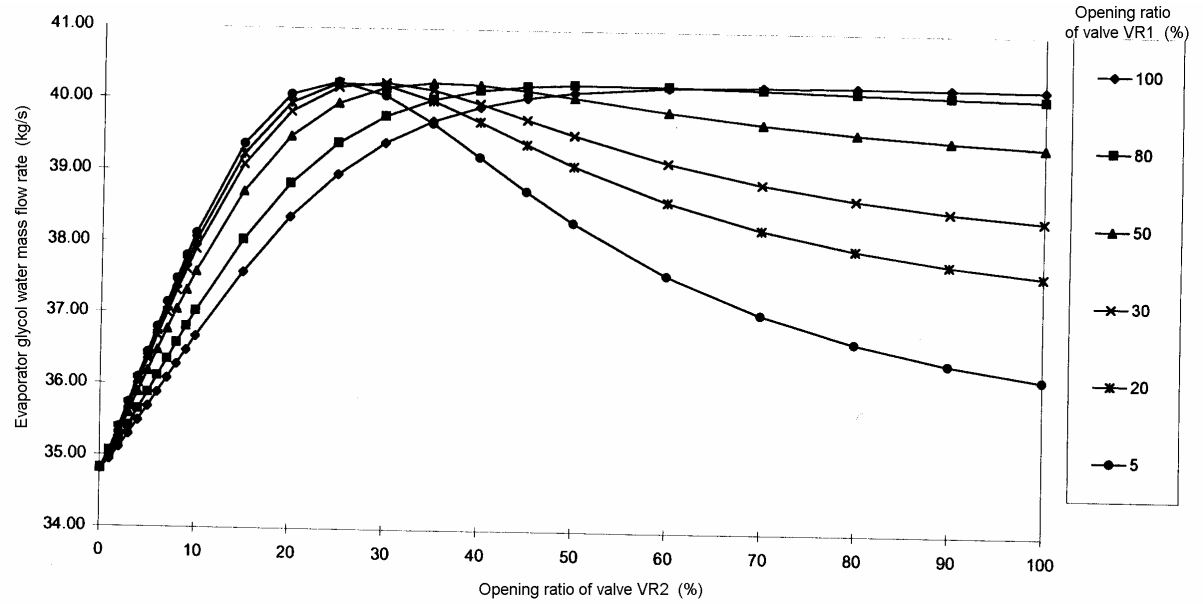

Figure 6 : evaporator glycol water mass flow rate (3 chillers, two primary pumps) - VR1 is the valve at the equilibrium tank exhaust and VR2 is the valve at the storage tank exhaust ; working domain : VR1 from 20 to 100 % and VR2 from 0 to 20 %

The nominal evaporator pump flow rate is equal to 32 kg s^{-1}. As it is shown in Table 2 and Figure 6, the hydraulic simulation gives a evaporator glycol water flow rate higher than the nominal value.

5. MODELING AND PERFORMANCE ANALYSIS OF THE TWIN-SCREW CHILLERS

5.1. The model of twin-screw chiller

The four twin-screw chillers are identical and use R22 as refrigerant. Each chiller is sized for a nominal refrigerating capacity of 960 kW in direct production mode and 700 kW in storage mode. Their condenser and evaporator are shell-and-tube heat exchangers, with three and two passes respectively.

Polynomial curve fits are used to represent the thermal performance of the chillers on the basis of the data provided by the manufacturer in full-load and part-load regimes (Pimenta, 1997).
Focus is given here on the full-load regime. The manufacturer's data show that, in the domain considered, the cooling capacity and the power consumed by the compressor are mainly influenced by the changes of glycol water temperature at the evaporator exhaust and the changes of water temperature at the condenser supply, while the effects of flow rate variations are comparatively negligible.

On the basis of these considerations, two polynomial curves are defined to represent the evolution of the cooling capacity (Q_{ev_FL}) and the compressor power consumption (W_{FL}) in full-load regime. They are function of the glycol water temperature at the evaporator exhaust and the water temperature at the condenser supply :

$$\begin{aligned} Q_{ev\_FL} = {} & (a_0 + a_1 T_{w,su,cd} + a_2 T_{w,su,cd}^2) + \\ & + \left(b_0 + b_1 T_{w,su,cd} + b_2 T_{w,su,cd}^2\right) T_{g,ex,ev} + \\ & + \left(c_0 + c_1 T_{w,su,cd} + c_2 T_{w,su,cd}^2\right) T_{g,ex,ev}^2 \end{aligned} \qquad (2)$$

$$\begin{aligned} W_{FL} = {} & (a_0 + a_1 T_{w,su,cd} + a_2 T_{w,su,cd}^2 + a_3 T_{w,su,cd}^3) + \\ & + \left(b_0 + b_1 T_{w,su,cd} + b_2 T_{w,su,cd}^2 + b_3 T_{w,su,cd}^3\right) T_{g,ex,ev} + \\ & + \left(c_0 + c_1 T_{w,su,cd} + c_2 T_{w,su,cd}^2 + c_3 T_{w,su,cd}^3\right) T_{g,ex,ev}^2 \end{aligned} \qquad (3)$$

The coefficients a_0,....,a_2, b_0,...,b_2, and c_0,...,c_2 are obtained by the least-square-fit method. For the cooling capacity, a good agreement (relative error = ± 1.8 %) is reached between polynomial results and manufacturer's data. For the compressor power consumption, the relative error ranges between ± 3.6 %.

5.2. Analysis of the thermal performance of the chillers

This analysis is still being performed. Since all the results are not available yet, this paper presents the methodology considered.

During a few months, the data provided by the control display of the chillers have been stored.
The data associated with the direct production mode (with/without discharge) have then be separated from the data related to the storage mode, due to the difference of the glycol water temperature (positive in the first mode and negative in the second one) and flow rate levels.

The thermal performance analysis of each operating mode is divided into two parts. The first one considers all the data available on the chillers. For example, for each chiller in full-load, the cooling capacity, the power consumed by the compressor, the evaporating and condensing pressures are plotted as function of the time. This allows one to point out some tendency over a long time period.
The second part deals with the analysis of the working points in steady-state regime. On the basis of the data available, the steady-state operating periods are isolated. The cooling capacity and the power consumed by the compressor related to each chiller are plotted as a function of the slide valve opening. These curves can then be compared between them.
For each working point in full-load regime, the "measured" cooling capacity and power consumed by the compressor is compared to the results of the chiller model. Since this static chiller model is based on the data provided by the manufacturer, this comparison allows one to check if the "measured" thermal performance is in good agreement with the performance foreseen by the manufacturer.

In the chiller performance analysis, the "measured" cooling capacity provided by the chillers is given by the following equation:

$$\dot{Q}_{ev} = \dot{M}_g \; c_g \; (t_{g,su,ev} - t_{g,ex,ev}) \qquad (4)$$

where $\dot{M}_g$ 3 is the evaporator glycol water mass flow rate ;
c_g is the glycol water specific heat ;
$t_{g,su,ev}$ is the glycol water temperature at the evaporator supply ;
$t_{g,ex,ev}$ is the glycol water temperature at the evaporator exhaust.

The evaporator glycol water flow rate is provided by the hydraulic analysis (see section 4) while the glycol water temperatures are provided by the control display of the chillers.
From the analysis of the data from the BEMS, it is observed that, in storage mode, the valve at the storage tank exhaust is modulating from 0 to 20 % and that, most of time, three chillers are used with two primary pumps. Therefore, for simplification purpose, a constant evaporator glycol water flow rate is considered for the analysis of the chiller performance in this operating mode. This flow rate is equal to 37.5 kg s^{-1} i.e. the average value of the flow rates shown in Figure 6 (the maximum value is 40.1 kg s^{-1} and the minimum value is 34.8 kg s^{-1}). But it should be noted that this simplification tends to underestimate the glycol water flow rate, and thus the "measured" cooling capacity, when the data analyzed is associated with the use of less than three chillers.

The “measuerd” power consumed by the compressor is given by the following simplified equation :

$$\dot{W} = \sqrt{3}\ U_{nom}\ I_{nom}\ \cos\phi\ \frac{FLA}{100} \qquad (5)$$

where U_{nom} is the nominal potential difference of the compressor motor (400V)
I_{nom} is the nominal and maximum current intensity allowed by the motor (280A)
cosΦ is the power factor (assumed to be equal to 0.9)
FLA is the ratio between the intensity of the current crossing the motor and the nominal current intensity (%). This information is provided by the control display of the chillers.

Assuming that the potential difference of the compressor motor and the power factor remain constant are crude hypotheses, but the FLA is the only information that can be recorded.

6. SIMULATION OF THE WHOLE COOLING PLANT

In addition to the analysis of the chiller thermal performance, the simulation of the cooling plant behavior in its different operating modes (direct production, discharging, etc.) is done using TRNSYS, a modular simulation software (Klein et al., 1994).

Each developed simulation file contains a detailed description of the inputs required, outputs provided as well as the units and the assumptions considered. The simulation files are set together to form a simulation software. This software, called TRNSED, is a limited version of TRNSYS. It also runs under Windows and is not submitted to any copyright.

The following section shows how the simulation of the cooling plant in pure discharging mode is validated.

6.1. The simulation of the discharging mode

The inputs required for the simulation of the discharging mode are :

- the initial nodule temperature in the ice storage tanks ;
- the number of operating primary and secondary pumps ;
- the opening ratios of the modulating valves at the storage tank exhaust and at the equilibrium tank exhaust ;
- the building cooling demand.

The simulation software mainly calculates the mass flow rates through the components, the fluid temperatures at the component supply and exhaust, the cooling capacity provided by the ice storage tanks, the cooling energy extracted from the tanks since the beginning of the simulation and the pump power consumption.

Two components need to be simulated in discharging mode : the ice storage tanks and the plate heat exchangers.

6.2. The model of plate heat exchanger

The plate heat exchangers are operating in counterflow arrangement. Each heat exchanger has a heat transfer surface of 116 m³ and a nominal power of 986 kW, for a mass flow rate of 30.7 kg/s and 37.5 kg/s for the cold water and the glycol water respectively, with a LMTD about 6.7 K.

The plate heat exchangers are modeled as classical counterflow heat exchangers. They are characterized by one parameter : their global heat transfer coefficient. These coefficients are assumed to be function of the thermal resistance on the cold water side, the thermal resistance of the metal and the thermal resistance on the glycol water side :

$$\frac{1}{AU} = R_w + R_m + R_g \qquad (6)$$

where AU is the global heat transfer coefficient of the heat exchanger ($W\ K^{-1}$);
R_w is the thermal resistance on the cold water side ($K\ W^{-1}$);
$R_w = c_1 \cdot (M_w)^{-0.8}$
R_m is the thermal resistance of the metal ($K\ W^{-1}$);
R_g is the thermal resistance on the glycol water side ($K\ W^{-1}$);
$R_g = c_2 \cdot (M_g)^{-0.8}$

The coefficients c_1, c_2 and R_m are identified on the basis of data provided by the manufacturer (Bourdouxhe, 1996).

6.3. The model of ice storage tank

The ice storage tanks are used in a parallel-series arrangement. Each tank has an internal volume of 58 m³, filled spherical capsules of a diameter of 95 mm. Each cubic meter of the tank volume contains an average of 1320 capsules. The flow direction and rate of the water-glycol across the tanks will be different as the tanks are charged or discharged. The maximum amount of cooling energy which can be stored, for a temperature decrease of the glycol water of 8 °C, is about 14000 kWh.

The model of encapsulated ice storage tank (Bilas, 1995) is based on the following assumptions :

- The tank is horizontally divided into sub-volumes where the water temperature in the spheres is assumed uniform;

- During the charging phase, the water temperature in the spheres of each sub-volume decreases till 0°C before freezing occurs. The temperature remains then equal to 0°C during the freezing of all the water in the spheres. After that, the water temperature can become negative. During the discharging phase, the opposed evolution is considered;

- In charging phase, the increase of the heat transfer coefficient due to partial crystallization is not accounted for;

- During freezing, the presence of water between the sphere wall and the ice is neglected ; the development of ice is assumed to be symmetric (from the sphere wall to its center) ; the effect of air in the sphere is neglected ; the increase of sphere volume during the freezing is neglected ; the effect of super cooling is accounted for ; the resistance through the liquid water in the sphere is neglected;

- During melting, the natural convection in water is neglected ; the decrease of sphere volume is neglected ; the effect of air in the sphere is neglected.

The purpose of the ice storage tank is to calculate the glycol water temperature at the exhaust of each sub-volume, the ice content and the water temperature in each sub-volume :

a) When the water temperature is higher or lower than 0 °C, the water contained in all the spheres is assumed to be respectively in liquid or solid state only. The water temperature is given by the following equation :

$$\frac{dT}{d\tau} = \frac{\varepsilon \dot{V}_g \rho_g c_g (T_{g_{su}} - T)}{V_{sub-vol} c_{vol}} \qquad 5(7)$$

where T is the water temperature (°C)

τ is the time (hr)

$\varepsilon = 1 - e^{-NTU}$

$$NTU = \frac{AU}{M_g c_g} \quad 6$$

M_g 7 is the glycol water mass flow rate in the sub-volume (kg s^{-1})

$AU = AU_{vol} . V_{sub-vol}$

AU_{vol} is the heat transfer coefficient per m^3 of sub-volume (W K^{-1} m^{-3}). This coefficient is calculated for water in liquid state and for water in solid state. Both values are assumed to remain constant.

$V_{sub-vol}$ is the volume of the sub-volume considered (m^3)

$\dot{V}_g$ 8 is the glycol water volume flow rate in the sub-volume (m^3 hr^{-1})

ρ_g is the glycol water density (1053 kg m^{-3})

c_g is the glycol water specific heat (3700 J kg^{-1} K^{-1})

$T_{g_{su}}$ 9 is the glycol water temperature at the sub-volume supply (°C)

c_{vol} is the liquid water or ice specific heat per m^3 of sub-volume (2273 10^3 J K^{-1} m^{-3} for liquid water and 1115 10^3 J K^{-1} m^{-3} for ice)

b) When the water temperature is equal to 0 °C, freezing or melting is occurring in all the spheres. The ice content in the spheres is given by the following equation :

$$\frac{dx}{d\tau} = \frac{\varepsilon \dot{V}_g \rho_g c_g (T_{g_{su}} - T)}{h_{fg,vol} V_{sub-vol}} \quad 10 \qquad (8)$$

where x is the ice content (fraction; $0 < x < 1$)

ε $= 1 - e^{-NTU}$

T is equal to 0°C

$h_{sf, vol}$ is the latent heat of ice per m^3 of sub-volume ($174\ 240\ 10^3$ J m^{-3})

AU $= AU_{vol} \cdot V_{sub\text{-}vol}$

During freezing : $AU_{vol} = 2500 + 2500\ x - 4400\ x^2$. This expression of the heat transfer coefficient per m^3 of sub-volume has been identified on the basis of the information given by the manufacturer.

During melting : $$AU_{vol} = N_{sphere} \left(\frac{1}{R_{1_{tot}}} + \frac{1}{R_{2_{tot}}} \right)$$

N_{sphere} is the number of spheres per m^3 of sub-volume. This value is estimated by the manufacturer.

$R_{1_{tot}}$ is the global thermal resistance characterizing the heat transfer between the glycol water and the ice (K W^{-1})11

$R_{2_{tot}}$ is the global thermal resistance characterizing the heat transfer between the glycol water and the liquid water in the sphere (K W^{-1})12

1314 $$R_{1_{tot}} = \frac{R_{ext} + \frac{e_{wall}}{k_{wall}}}{S_{wall\text{-}ice}} \quad 15$$

$$R_{2_{tot}} = \frac{R_{ext} + \frac{e_{wall}}{k_{wall}} + \frac{e_{water}}{k_{water}}}{S_{wall\text{-}water}} \quad 1617$$

$$R_{ext} = \frac{D_{Sphere}}{C\ k_g}\ \mathrm{Re}^{-0.5}\ \mathrm{Pr}^{-0.33}$$

R_{ext} is the thermal resistance characterizing the heat transfer between the glycol water and the sphere wall (K m^2 W^{-1})

$S_{wall\text{-}ice}$ is the contact surface 18between ice and the sphere wall (m^2)

$S_{wall\text{-}water}$ is the contact surface 19between liquid water and the sphere wall (m^2)

e_{wall} is the sphere wall thickness (m)

k_{wall} is the sphere wall thermal conductivity (0.33 W m^{-1} K^{-1})

e_{water} is the mean thickness of the liquid water film in the sphere (m)

k_{water} is the liquid water thermal conductivity (0.6 W m^{-1} K^{-1})

$D_{sphère}$ is the sphere diameter (m)

C is a constant. The value of this constant has been identified on the basis of the data given by the manufacturer (-)

k_g is the glycol water thermal conductivity (0.480 W m^{-1} K^{-1})

Re is the Reynolds number (-)

Pr is the Prandtl number (-)

c) The glycol water temperature at the sub-volume exhaust is given by the following equation which accounts for the time needed by the glycol water flow to cross the sub-volume :

$$T_{g_{ex}} = T_{ex} - (T_{ex} - T_{g_{ex,i}})\ e^{-\frac{\Delta\tau}{\tau_g}} \quad 20 \qquad (9)$$

where $T_{g_{ex}}$ 21 is the "actual" glycol water temperature at the sub-volume exhaust (°C)

T_{ex} represents the static glycol water temperature at the sub-volume exhaust (°C)

$$T_{ex} = T_{g_{su}} - \varepsilon (T_{g_{su}} - T) \quad 22$$

$\Delta\tau$ is the time step (hr)

τ_g represents the time needed by the glycol water flow to cross the sub-volume. It is defined by the ratio between the glycol water volume in the sub-volume and the glycol water volume flow rate. The manufacturer estimates that 40 % of the ice storage volume is occupied by the glycol water.

$T_{g_{ex,i}}$ 23 is the glycol temperature at the tank exhaust at the previous time step (°C)

6.4. The validation of the simulation of the discharging

A discharging test was carried out during an afternoon in order to check the performance of the ice storage system. The night preceding the test, the chillers were used to charge the ice storage tanks up to their maximum capacity.
The morning of the test day, air handling units were put into use in order to increase the building cooling demand up to about 2 MW. The thermal simulation of all the air handling units in use allowed the checking of the values given by the enthalpy flow meters (Hu, 1996). During this preparation phase, only the chillers were being used. At the beginning of the afternoon, the chillers were switched off and the discharging test began.

During the discharging test, two primary and secondary pumps are used and the modulating valve at the storage tank exhaust (VR2) is opened progressively while the opening ratio of the modulating valve at the equilibrium tank exhaust (VR1) remains constant (see Figure 7).

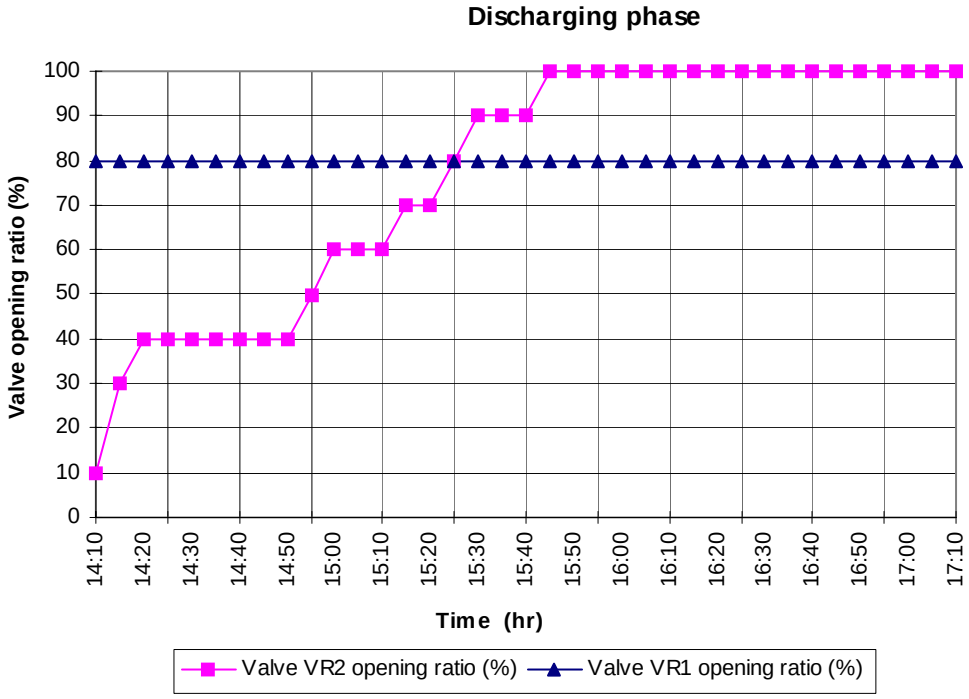

Figure 7 : Evolution of the Valve Opening Ratio at the Storage Tank Exhaust (VR2) and at the Equilibrium Tank Exhaust (VR1) (data given by the BEMS)

Figure 8 shows the measured water temperature at the building supply and exhaust, the total cold water flow rate as well as the cold water enthalpy flow rates measured by the enthalpy fllow meters.

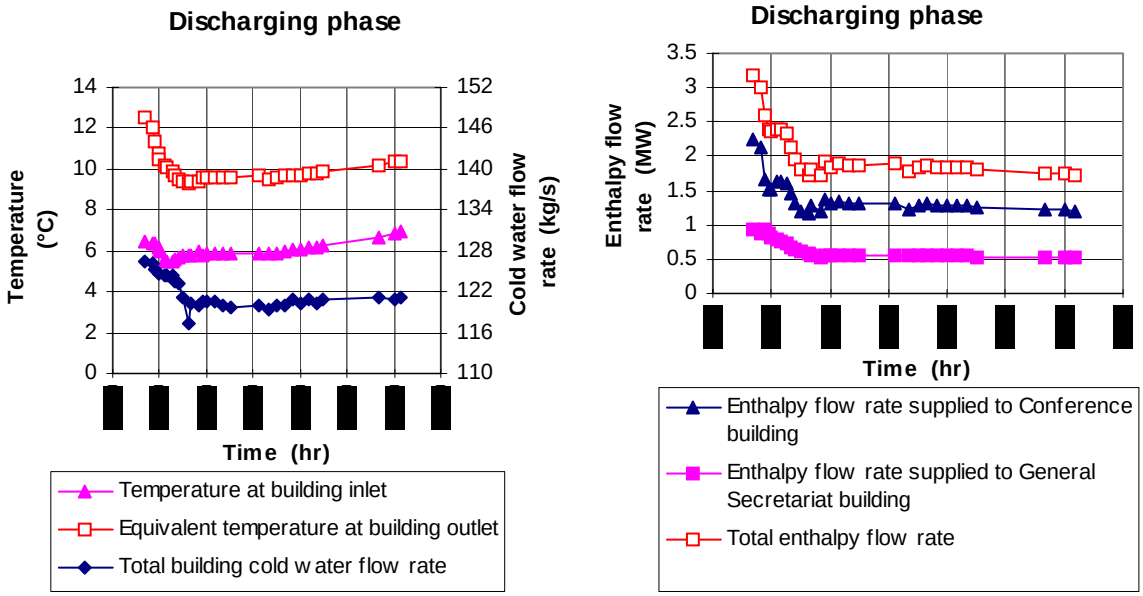

Figure 8 : Evolution of the Cold Water Temperatures, the Total Cold Water Flow Rate and the Cold Water Enthalpy Flow Rates Given by the Enthalpy Flow Meters

The initial peak of enthalpy flow rate (see Figure 8) corresponds to the transition between the chiller use and the storage tank use. During this transient period, the cold water network is cooled down to approximately 6 °C at the building supply. This temperature remains very stable from 14h45 to 16h50. After this period of stability, the cold water temperatures begins to increase smoothly, meaning that the ice storage tanks, in these operating conditions, are no more able to meet the cooling demand of the building.

The last input needed by the simulation of the discharging is the initial nodule temperature in the ice storage tanks. The ice storage tank model assumes that, at the beginning of the discharging phase, the temperatures of glycol water and water in the spheres are equal and uniform. This initial temperature is assumed to be given by the sensor located at the ice storage tank exhaust .
However, the checking of the data provided by the BEMS showed that the temperature given by this sensor was obviously too low (about 4 °C). Therefore, two simulations have been performed : the first one uses the temperature given by the sensor as initial temperature in the storage tanks (Ti = -9.6 °C) while the second simulation considers an initial temperature equal to -6 °C.

Figure 9 compares the glycol water temperature at the ice storage tank exhaust provided by both simulations and by the data acquisition system.

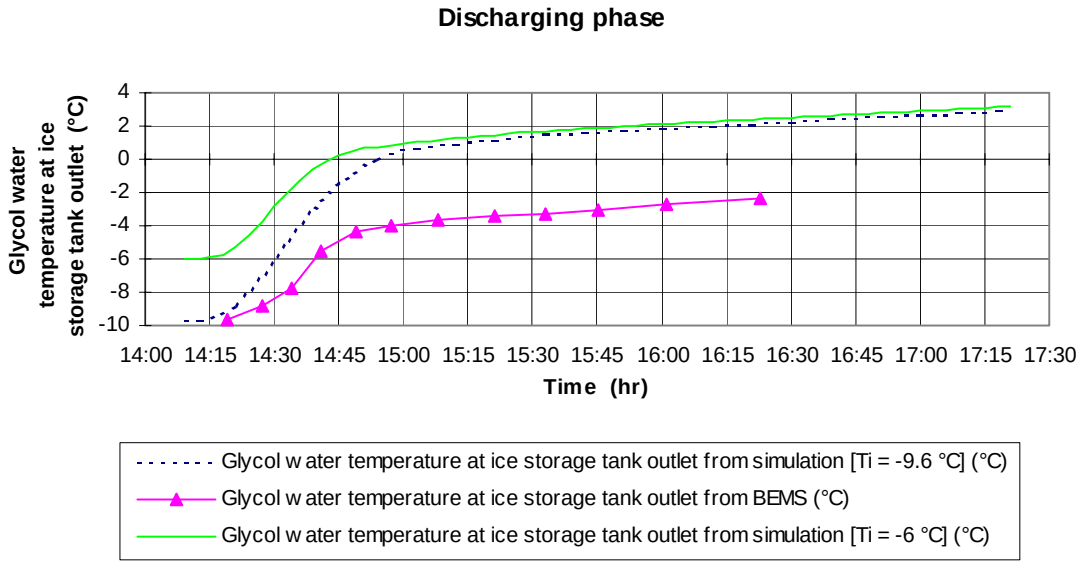

Figure 9 : Glycol Water Temperature at the Ice Storage Tank Exhaust

As it is shown by Figure 9, there is a nearly constant difference between the temperature provided by the simulation using -6 °C as initial temperature in the tanks and the temperature provided by the BEMS. The curves provided by the simulations coincide after one hour of discharge. This means that, after one hour, the cooling capacity is essentially provided by the melting of ice. As a logical consequence, the glycol water flow leaves the storage tanks at a temperature slightly above 0 °C. These results point out that the sensor at the ice storage tank exhaust gives obviously a too low temperature (about 4 °C). This is in good agreement with the measurement made manually at the end of the discharging test.
Figure 10 compares the glycol water temperature at the heat exchanger supply provided by both simulations and by the data acquisition system.

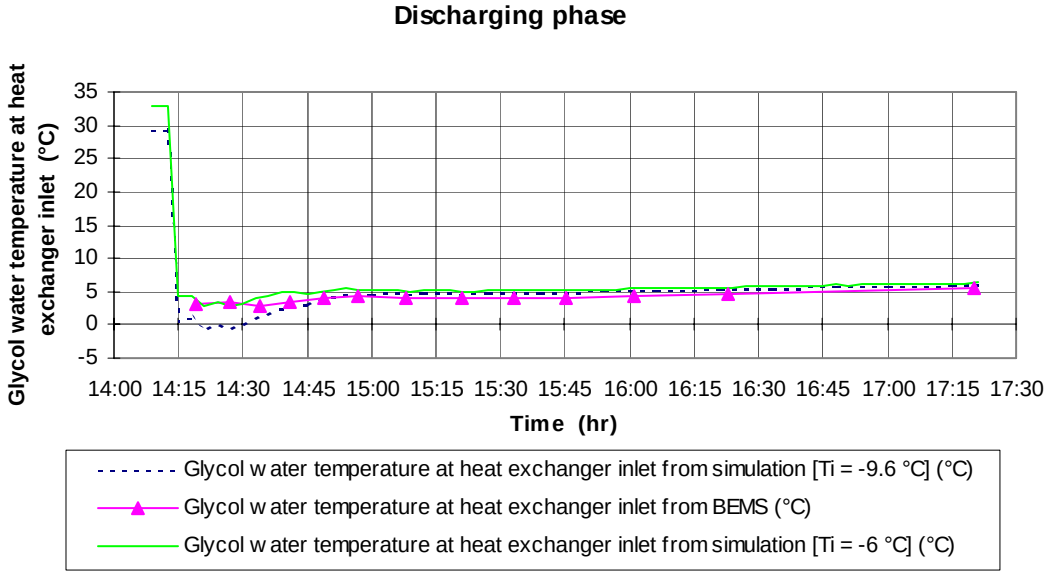

Figure 10 : Glycol Water Temperature at the Heat Exchanger Supply

As it is shown by Figure 10, there is a very satisfactory agreement between the simulation results and the data provided by the BEMS, except during the first ten minutes of discharge. But, during this time period, very few information was available about the cooling loads so that they were roughly approximated. As in Figure 9, the curves provided by the simulations coincide after one hour of discharge. One can also remark that, at the beginning of the discharging test, the results given by the simulation using -6 °C as initial temperature in the storage tanks are in better agreement with the data provided by the BEMS. This confirm again the inaccuracy of the sensor located at the storage tank exhaust.
Figure 11 compares the cold water temperature at the building supply provided by both simulations and by the data acquisition system.

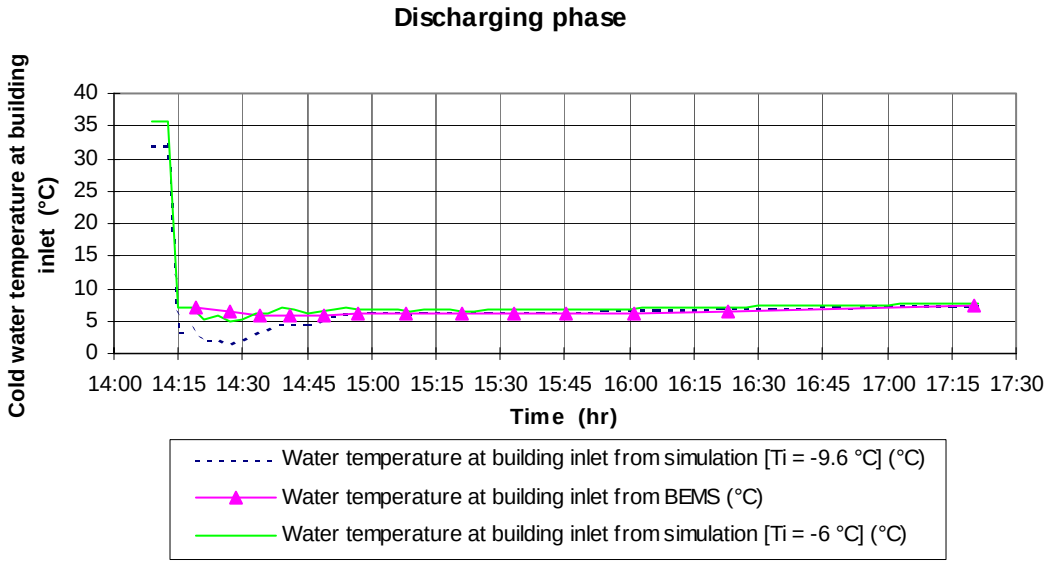

Figure 11 : Cold Water Temperature at the Buidling Supply

Such as for Figure 10, Figure 11 shows a very satisfactory agreement between the simulation results and the data provided by the BEMS, except during the first ten minutes of discharge. The simulation results also show the increase of cold water temperature during the last hour of discharging test. This temperature drift means that the ice storage tanks can no longer meet the building cooling loads (1.8 MW during the whole discharging test) while satisfying the set point water temperature at the building supply (7 °C). This is due to the fact that, during the test, the opening ratio of the modulating valve at the equilibrium tank exhaust had to be above 80 % to avoid cavitation in the glycol water pumps.

7. CONCLUSIONS AND RECOMMENDATIONS

The analysis of the data provided by the acquisition system points out the inaccuracy of several sensors. This uncertainty reduces strongly the accuracy of the thermal and mass balances.

The hydraulic analysis mainly based on the data provided by the installers and the manufacturers allows one to reduce the uncertainty on the flow rates, but it does not solve the whole problem. Since the hydraulic simulation needs to be adjusted on the basis of the results of the thermal balances, the calibration of the sensors of the acquisition system would increase the quality of this adjustment and thus of the simulation. Of course, a series of flow rate measurements would also improve the results of the hydraulic analysis.

The simulated flow rates and the data provided by the control display of the chillers are used to evaluate the thermal performance of the chillers. This analysis is still being performed. It compares the “measured” thermal performance of the four chillers, but also compares the “measured” thermal performance of each chiller in stable full-load regime with the performance provided by the chiller model. This chiller model is a polynomial model developed on the basis of the data supplied by the manufacturer.
Of course, the “measured” cooling capacity and power consumption directly depend on the accuracy of the temperature sensors and of the hydraulic analysis. The reliability of the analysis of the chiller performance would therefore be improved thanks to a calibration of the sensors or, better, thanks to flow rate measurements.

Several simulation files are developed to simulate the different operating modes of the cooling plant. The simulation of the pure discharging mode is based on the modeling of the ice storage tanks and of the plate heat exchangers. Here again, the models are identified on the basis of the data provided by the manufacturers. A discharging test allowed the simulation of this operating mode to be successfully validated.

8. ACKNOWLEDGMENTS

This study is supported by the General Secretariat of the European Union.

9. REFERENCES

ASHRAE. 1995. ASHRAE Applications Handbook—Chapter 40 : thermal storage. American Society of Heating, Refrigerating and Air-conditioning Engineers. Atlanta.

Bilas F. 1995. ANALYSE DE LA CENTRALE DE FROID DU BATIMENT CONFERENCE DESTINE AU CONSEIL DES COMMUNAUTES EUROPEENNES A BRUXELLES. Travail de fin d'études. University of Liege. Belgium.

Bourdouxhe J-P. 1996. Detailed analysis of HVAC subsystem. WD-75. Working document of the IEA-Annex 30 “Bringing to application”

CEE-CLIM .1995a. CALCULS HYDRAULIQUES DE LA CENTRALE DE FROID MODIFIEE. Rapport interne CEE.

CEE-CLIM. 1995b . RAPPORT DE MISE EN SERVICE DES CIRCUITS DE LA CENTRALE DE FROID. Rapport interne CEE.

Hu H. 1996. Analysis of an air-conditioning system. Thesis submitted to the requirement for the degree of Master of Applied Sciences. University of Liege.

Jennes V. 1996. ANALYSE DE LA CENTRALE DE FROID DU BATIMENT DES COMMUNAUTES EUROPEENNES A BRUXELLES. ETUDE DES TOURS DE REFROIDISSEMENT ET DU CIRCUIT HYDRAULIQUE ASSOCIE: MODELISATION, VALIDATION, SIMULATION. Travail de fin d'études. University of Liege. Belgium.

Klein et al. 1994. TRNSYS : A Transient System Simulation Program. Solar Energy Laboratory, University of Madison, U.S.A.

Pimenta. 1997. On the suitability of simple methods for fault detection and diagnosis. Laboratory tests and on-site studies of refrigeration systems. Thesis to be submitted to the requirements for the degree of Doctor of Applied Sciences.